MEDICAL SCIENCE MONITOR

LAB/IN VITRO RESEARCH

e-ISSN 1643-3750
© Med Sci Monit, 2020; 26: e924160
DOI: 10.12659/MSM.924160

Received: 2020.03.10
Accepted: 2020.05.06
Available online: 2020.06.03
Published: 2020.07.28

CircKIAA0907 Retards Cell Growth, Cell Cycle, and Autophagy of Gastric Cancer *In Vitro* and Inhibits Tumorigenesis *In Vivo* via the miR-452-5p/KAT6B Axis

Authors' Contribution:
Study Design A
Data Collection B
Statistical Analysis C
Data Interpretation D
Manuscript Preparation E
Literature Search F
Funds Collection G

BCDE 1 Lingyu Zhu
CDEF 1 Chunfei Wang
BCDE 2 Shengquan Lin
ABCD 1 Lei Zong

1 Department of Gastroenterology, Weifang People's Hospital, Weifang, Shandong, P.R. China
2 Department of Pain, Weifang People's Hospital, Weifang, Shandong, P.R. China

Corresponding Author: Lei Zong, e-mail: tup7yzi@163.com
Source of support: Departmental sources

Background: The significant roles of circular ribonucleic acids (RNAs) in cancers have been discussed in many studies. This report aimed to investigate the biological functions of circKIAA0907 and its action mechanism in gastric cancer (GC).

Material/Methods: Relative RNA expression levels were determined using quantitative real-time polymerase chain reaction (qRT-PCR). The examination of cell proliferation was performed via 3-(4, 5-dimethylthiazol-2-y1)-2, 5-diphenyl tetrazolium bromide assay. Flow cytometry was used to analyze the apoptosis rate and cell cycle. Protein levels were quantified using western blot. Biotinylated RNA pull-down assay was used to find the microRNA target of circKIAA0907; target binding was validated through dual-luciferase reporter assay. The assay *in vivo* was executed via a xenograft tumor model to explore the role of circKIAA0907 in GC.

Results: CircKIAA0907 was downregulated in GC and had higher stability than its linear isoform. Functionally, circKIAA0907 upregulation resulted in the repression of proliferation, cell cycle, and autophagy and promotion of apoptosis in GC cells. Mechanistically, circKIAA0907 bound to miR-452-5p as a specific sponge for it; lysine acetyltransferase 6B (*KAT6B*) was a target gene of miR-452-5p, so circKIAA0907 elevated KAT6B levels via sponging miR-452-5p. Reversion assays indicated that circKIAA0907 served as a tumor inhibitor by inhibiting miR-452-5p and increasing KAT6B; miR-452-5p inhibition impeded GC development by upregulating KAT6B. The miR-452-5p/KAT6B axis was also accountable for circKIAA0907-induced tumorigenesis suppression *in vivo*.

Conclusions: This work demonstrated that circKIAA0907 has diagnostic and therapeutic value in GC by acting as an oncogenic molecule via the miR-452-5p/KAT6B axis.

MeSH Keywords: Cell Migration Inhibition • Cell Proliferation • Stomach Neoplasms

Full-text PDF: https://www.medscimonit.com/abstract/index/idArt/924160

3612 — 8 32

This work is licensed under Creative Common Attribution-NonCommercial-NoDerivatives 4.0 International (CC BY-NC-ND 4.0)

Indexed in: [Current Contents/Clinical Medicine] [SCI Expanded] [ISI Alerting System] [ISI Journals Master List] [Index Medicus/MEDLINE] [EMBASE/Excerpta Medica] [Chemical Abstracts/CAS]

Background

Gastric cancer (GC) is the third leading cause of cancer-related death around the world, with high incidence in eastern Asia [1]. Unfortunately, there is no efficient screening method to detect early GC because of its symptom-free nature; hence most patients are diagnosed with advanced-stage GC [2]. Understanding the functional and molecular mechanisms of GC pathogenesis would be considerably significant in monitoring the development of GC and identifying biomarkers for diagnosis, treatment, and prognosis [3].

Circular ribonucleic acids (circRNAs) are covalently closed-loop structures and function as crucial regulatory molecules in cancer oncogenesis [4,5]. Li et al. proved that circRNA CDR1as was an oncogenic factor in nonsmall-cell lung cancer [6], and Lin and Cai claimed that circ-EGLN3 enhanced the proliferation and aggressiveness of renal cell carcinoma cells [7]. Circ_LARP4 was shown to inhibit ovarian cancer cell proliferation and migration [8], and the anticancer role of circMTO1 was demonstrated in rectal cancer [9]. Many dysregulated circRNAs have been found in GC tissues [10], including the downregulated circKIAA0907 (has_circ_0005758) [11]. However, whether circKIAA0907 is an oncogene or inhibitor in GC remains unexplored.

MicroRNAs (miRNAs), another class of posttranscriptional regulators, are also involved in diverse cellular processes of cancers by interacting with the 3' untranslated regions (3'-UTRs) of target genes [12]. Increasing evidence determined that circRNAs acted as "miRNA sponges" to regulate genes [13]. MiR-452 was upregulated and contributed to the biological carcinogenesis of GC through targeting EPB41L3 [14]. We speculated that miR-452-5p (a subunit of miR-452) had the same effect on GC, and that circKIAA0907 might act as a sponge of miR-452-5p.

The downstream targets for miR-452-5p in GC are unreported. Lysine acetyltransferase 6B (KAT6B) has regulatory effects on many cancers, such as oncogenic function in prostate cancer [15] and an inhibitory role in small-cell lung cancer [16]. Low expression of KAT6B was reported in GC; it was a target of miR-4513 in GC cells [17]. Here, the relation between KAT6B and miR-452-5p is researched.

In this study, we analyze the biological role of circKIAA0907 and its relation with miR-452-5p and KAT6B and reveal its role in GC pathogenesis.

Material and Methods

Tumor samples and cell culture

Tumor tissues (n=47) were gathered from informed GC patients during gastrectomy at Weifang People's Hospital, and the peritumoral tissues (n=47) were collected as normal controls. Instantly, these samples were submerged in liquid nitrogen to stay fresh for subsequent RNA isolation. Written informed consent was given by each patient and the current research was ratified by the Ethics Committee of Weifang People's Hospital (approval Sept. 18th 2018).

Human gastric epithelial cell line GES-1 and GC cell lines (HGC27, AGS, MKN45, and NCIN87) from GOBIOER (Nanjing, China) were grown in culture medium consisting of basic RPMI-1640 medium, 10% fetal bovine serum, and 1% antibiotics (10,000 U/mL of penicillin and 10,000 µg/mL of streptomycin). These culture-related reagents were all bought from Gibco (Carlsbad, CA, USA). Cells in the culture flask were placed in a humidified incubator (Thermo Fisher Scientific, Waltham, MA, USA) with controlled temperature at 37°C and CO_2 at 5%. Cells were subcultured every 3 days at a ratio of 1: 3.

Cell transfection

Using the circRNA expression vector pCE-RB-Mam (RIBIBIO, Guangzhou, China), the recombinant vector pCE-RB-Mam-circKIAA0907 (circKIAA0907) was constructed. The miR-452-5p mimic and inhibitor (miR-452-5p and anti-miR-452-5p), miRNA mimic- and inhibitor-negative controls (miR-NC and anti-miR-NC), and small interfering RNA (siRNA) targeting KAT6B (si-KAT6B) and siRNA NC (si-NC) were also obtained from RIBIBIO. Monolayers of HGC27 and AGS cells were transfected with the above vectors and oligonucleotides via the Lipofectamine3000 (Invitrogen, Carlsbad, CA, USA) according to the supplied guidelines for users.

Quantitative real-time polymerase chain reaction (qRT-PCR)

TRI reagent (Sigma, St. Louis, MO, USA) was used for extracting the total RNA from GC tissues and cells. Nuclear and cytoplasmic RNA were isolated via the PARIS™ kit (Invitrogen) following the manufacturer's instructions. RNA (2000 ng) was reversely transcribed into complementary deoxyribonucleic acid through Transcriptor high-fidelity reverse transcriptase (Roche, Basle, Switzerland), and the sample abundance was quantified by qRT-PCR using ABI7500 real-time PCR system (Applied Biosystems, Carlsbad, CA, USA) and FastStart SYBR qPCR mix (Roche). Analyses of all data were performed using the $2^{-\Delta\Delta Ct}$ method. Glyceraldehyde-3-phosphate dehydrogenase (*GAPDH*) was selected as a reference gene for the standardization of

This work is licensed under Creative Common Attribution-NonCommercial-NoDerivatives 4.0 International (CC BY-NC-ND 4.0)

Indexed in: [Current Contents/Clinical Medicine] [SCI Expanded] [ISI Alerting System] [ISI Journals Master List] [Index Medicus/MEDLINE] [EMBASE/Excerpta Medica] [Chemical Abstracts/CAS]

circRNA and messenger RNA (mRNA) levels, whereas U6 was used to normalize miRNA expression. Specific primers were synthesized from Sangon (Shanghai, China), including circKIAA0907:
Forward (F), 5'-ACCCACTCCTCCACCTTTGAC-3' and reverse (R), 5'-TGTTGCTGTAGCCAAATTCGTT-3';
KIAA0907: F, 5'-CCCTACGGAGTACCAAGCATAG-3' and R, 5'-CAGGAGCAGCAGGAATAAAAGGA-3';
miR-452-5p: F, 5'-AGCGCGAACTGTTTGCAGAGGA-3' and R, 5'-ATCCAGTGCAGGGTCCGAGG-3';
KAT6B: F, 5'-ATACGAGCGAATGGGTCAGAGTGATTTTGG-3' and R, 5'-GTTCACAGAGTTGACATTGTAGGCTGGCG-3';
GAPDH: F, 5'-CTTCAACAGCGACACCCA-3' and R, 5'-ATGAGGTCCACCACCCT-3';
U6: F, 5'-GCTTCGGCAGCACATATACTAAAAT-3' and R, 5'-CGCTTCACGAATTTGCGTGTCAT-3'.

Actinomycin D and ribonuclease R (RNase R) treatment

Actinomycin D (2 mg/mL) (Millipore, Billerica, MA, USA) was pipetted into the culture solution for GC cells and cells were harvested after incubation for 0, 4, 8, 12, and 24 h. Total RNA (4 μg) was mixed with 12 U of RNase R (3 U/μg; Epicentre Technologies, Madison, WI, USA) in a 37°C water bath for 1 h. Relative levels of circKIAA0907 and its linear isoform KIAA0907 were examined by qRT-PCR.

3-(4, 5-Dimethylthiazol-2-y1)-2, 5-diphenyl tetrazolium bromide (MTT) assay

After 24-h incubation of GC cells (about 1×10^4) inoculated into 96-well plates, cell transfection of different groups was carried out. After 0, 12, 24, and 48 h, 50 μL of 1×MTT (5×MTT diluted with dilution buffer; KeyGen, Nanjing, China) was added to each well to restore the formazan. Four hours later, the supernatant was aspirated and 150 μL/well of dimethyl sulfoxide (Invitrogen) was added to dissolve formazan. At a wavelength of 490 nm, the optical density was measured through a microplate reader (Thermo Fisher Scientific).

Flow cytometry

Cellular apoptosis was assessed using the double staining of Annexin V-fluorescein isothiocyanate (Annexin V-FITC) and propidium iodide (PI) via the eBioscience™ Annexin V-FITC apoptosis detection kit (Invitrogen). Cell suspension (195 μL) in 1× Bing buffer (6×10^4 cells) was added with 5 μL of Annexin V-FITC for 10 min. PI (10 μL) was added to the tube after cell washing and resuspension with 190 μL of binding buffer, whereafter the apoptotic cells (Annexin V+/PI- and Annexin V+/PI+) were discerned by flow cytometry (BD Biosciences, San Diego, CA, USA). The apoptosis rate was accurately calculated using the general formula: apoptotic cells/total cells × 100%.

Western blot

GC tissues and cells were lysed in radioimmunoprecipitation assay buffer (Sangon). Next, 35 μg of proteins were loaded on 10% Bolt™ Bis-Tris precast polyacrylamide gels (Invitrogen) to perform electrophoresis for 120 min. Then the separated proteins on the gels were moved onto polyvinylidene fluoride membranes (Millipore) through an electrotransfer apparatus, and then the membranes were immersed in 5% skim milk (Sangon) to block the binding of nonspecific proteins. After incubation with primary antibodies for 4 h and secondary antibodies for 1 h at room temperature, the combined specific protein complex was detected using ECL substrate kit (Abcam, Cambridge, UK) and target protein levels were analyzed by the ImageLab software version 4.1 (Bio-Rad, Hercules, CA, USA). Our antibodies were all purchased from Abcam: anti-B-cell lymphoma-2 (anti-Bcl-2; ab185002, 1: 1000), Bcl-2-associated X (anti-Bax; ab32503, 1: 1000), anti-light chain 3B (anti-LC3B; ab51520, 1: 1000), anti-p62 (ab109012, 1: 1000), anti-Beclin-1 (ab62557, 1: 1000), anti-KAT6B (ab58823, 1: 1000), anti-GAPDH (ab9485, 1: 3000), and anti-rabbit immunoglobulin G/horseradish peroxidase secondary antibody (ab205718, 1: 5000).

Cell cycle detection

Ice-cold 70% ethyl alcohol (Sangon) was used for fixing cells overnight at 4°C. After centrifugation (1000 revolutions per minute) for 5 min, cell pellets were resuspended in 50 μL of RNase A (Sangon) and incubated for 30 min at 37°C, followed by staining with 400 μL of PI (Sangon). Thirty minutes later, cells at different phases (G0/G1, S, and M) were analyzed via flow cytometry (BD Biosciences).

Biotinylated RNA pull-down assay

For circKIAA0907 pulled-down miRNAs, HGC27 and AGS cells were incubated with probe-coated beads after mixing of the biotinylated circKIAA0907 probe and C-1 magnetic beads (Life Technologies, Carlsbad, CA, USA) at 4°C overnight. Then qRT-PCR was used to determine the expression levels of different miRNAs. GC cells that overexpressed circKIAA0907 were transfected with wild-type (WT) biotinylated-miR-452-5p (Bio-miR-452-5p-WT) or its mutant mimic (Bio-miR-452-5p-MUT) and cell lysates were incubated with C-1 magnetic beads, followed by the detection of circKIAA0907 and GAPDH using qRT-PCR.

Dual-luciferase reporter assay

The circKIAA0907 sequences containing the WT (with the binding sites for miR-452-5p) or MUT (with the mutated sites for miR-452-5p) were singly amplified and cloned into the pGL3 luciferase basic vector (Promega, Madison, WI, USA), named as circKIAA0907 WT and circKIAA0907 MUT. Additionally,

This work is licensed under Creative Common Attribution-NonCommercial-NoDerivatives 4.0 International (CC BY-NC-ND 4.0)

Indexed in: [Current Contents/Clinical Medicine] [SCI Expanded] [ISI Alerting System] [ISI Journals Master List] [Index Medicus/MEDLINE] [EMBASE/Excerpta Medica] [Chemical Abstracts/CAS]

the KAT6B 3'-UTR-WT and KAT6B 3'-UTR-MUT were constructed after molecular cloning as above. Then cells were cotransfected with these vectors and miR-452-5p or miR-NC for 48 h and collected to determine luciferase activity via the dual-luciferase assay system (Promega). The relative luciferase activity was recorded after the standardization of renilla to firefly luciferase intensity.

Xenograft tumor assay

Six-week-old BALB/c nude mice (n=20) were bought from Shanghai Animal Experimental Center (Shanghai, China) and randomly divided into four groups. HGC27 and AGS cells (2×10^6) with the respective transfection of circKIAA0907 and vector were injected into the right side of the back of the mice, establishing the xenograft model *in vivo*. Subsequently, tumor length and width were measured by a digital caliper each week, and tumor volume was calculated by the formula: length×width squared ×0.5. At 35 days postinjection, tumors were weighed after excision from the euthanized mice. Expression of circKIAA0907, miR-452-5p, and KAT6B was determined with qRT-PCR and western blot. The Animal Ethics Committee of Weifang People's Hospital approved this experiment (approval Sept. 18th 2018).

Statistical analysis

All data are shown as mean±standard deviation on the basis of three independent biological parallels. SPSS 22.0 was used for statistical analyses and graphing was performed by GraphPad Prism 7. Differences were tested via Student's *t* test and one-way analysis of variance followed by Tukey's test. $P<0.05$ was deemed statistically significant.

Results

CircKIAA0907 expression was lessened in GC tissues and cells

CircKIAA0907 (hsa_circ_0005758) originates from exons 5 to 7 of the KIAA0907 gene located in chromosome 1: 155891165–155893478, and its spliced mature sequence length is 373 base pairs (Figure 1A). We used qRT-PCR to investigate its level in GC tissues and cells. As depicted in Figure 1B, circKIAA0907 expression in GC tissue was much lower than that in matched normal tissue. In GC (HGC27, AGS, MKN45, and NCIN87) cell lines, we observed the same result in comparison with normal GES-1 cells (Figure 1C). HGC27 and AGS cells, with more significant downregulation than MKN45 and NCIN87 cells, were used for the following research.

The assessment of circKIAA0907 stability and localization was then carried out. After treatment with actinomycin D (a transcription repressor), circKIAA0907 was shown to have a half-life exceeding 24 h, whereas linear KIAA0907 decreased to half at only 4 h posttreatment (Figure 1D, 1E). Compared with the RNase R- group, circKIAA0907 was more resistant to RNase R digestion than KIAA0907, affirming the high stability of circKIAA0907 (Figure 1F, 1G). According to qRT-PCR analysis, we found that circKIAA0907 was predominately located in the cytoplasm, contrasting with GAPDH (cytoplasm control) and U6 (nucleus control) (Figure 1H, 1I). These data imply that circKIAA0907 has the potential to be a tumor inhibitor.

Overexpression of circKIAA0907 triggered proliferation and autophagy inhibition, cell cycle arrest, and apoptosis promotion of GC cells *in vitro*

Exploring the potential role of circKIAA0907 in GC biology, we constructed the recombined vector containing the circKIAA0907 sequence to overexpress circKIAA0907. The expression of circKIAA0907 was increased more than 10-fold in HGC27 and AGS cells transfected with circKIAA0907 relative to the vector group (Figure 2A, 2B). As the result of circKIAA0907 overexpression, cell proliferation was distinctly restrained (Figure 2C, 2D), whereas the apoptosis rate was boosted (Figure 2E, 2F) in HGC27 and AGS cells. Western blot showed the decrease of Bcl-2 (anti-apoptosis protein) and elevation of Bax (a promoter of apoptosis) in the circKIAA0907 transfection group comparised with the vector group, also implicating apoptosis promotion by circKIAA0907 (Figure 2G, 2H). By performing cell cycle detection, we discovered that the upregulation of circKIAA0907 increased the proportion of the G0/G1 phase and reduced the S phase in HGC27 and AGS cells, causing cell cycle arrest (Figure 2I, 2J). Commonly, LC3B-II/I and Beclin-1 are identified to promote autophagy, whereas p62 can inhibit autophagy [18]. The decline of LC3B-II/I and Beclin-1 and the upregulation of p62 demonstrated that the overexpressed circKIAA0907 repressed autophagy of HGC27 and AGS cells (Figure 2K, 2L). These results together prove that circKIAA0907 impedes GC carcinogenesis *in vitro*.

CircKIAA0907 could sponge miR-452-5p in GC cells

It is unknown whether circKIAA0907 can act as sponges of miRNAs. We performed the biotinylated-circKIAA0907 pull-down assay to determine which miRNA among 8 candidate miRNAs (miR-203b-3p, miR-761, miR-16-1-3p, miR-296-3p, miR-31-5p, miR-377-5p, miR-452-5p, miR-503-3p) could interact with circKIAA0907. Our qRT-PCR analysis showed that the circKIAA0907 probe was able to pull down circKIAA0907 and the pull-down efficiency was improved after circKIAA0907 upregulation (Figure 3A, 3B). In HGC27 and AGS cells, miR-452-5p was the most evident miRNA between two miRNAs (miR-296-3p

This work is licensed under Creative Common Attribution-NonCommercial-NoDerivatives 4.0 International (CC BY-NC-ND 4.0)

Indexed in: [Current Contents/Clinical Medicine] [SCI Expanded] [ISI Alerting System] [ISI Journals Master List] [Index Medicus/MEDLINE] [EMBASE/Excerpta Medica] [Chemical Abstracts/CAS]

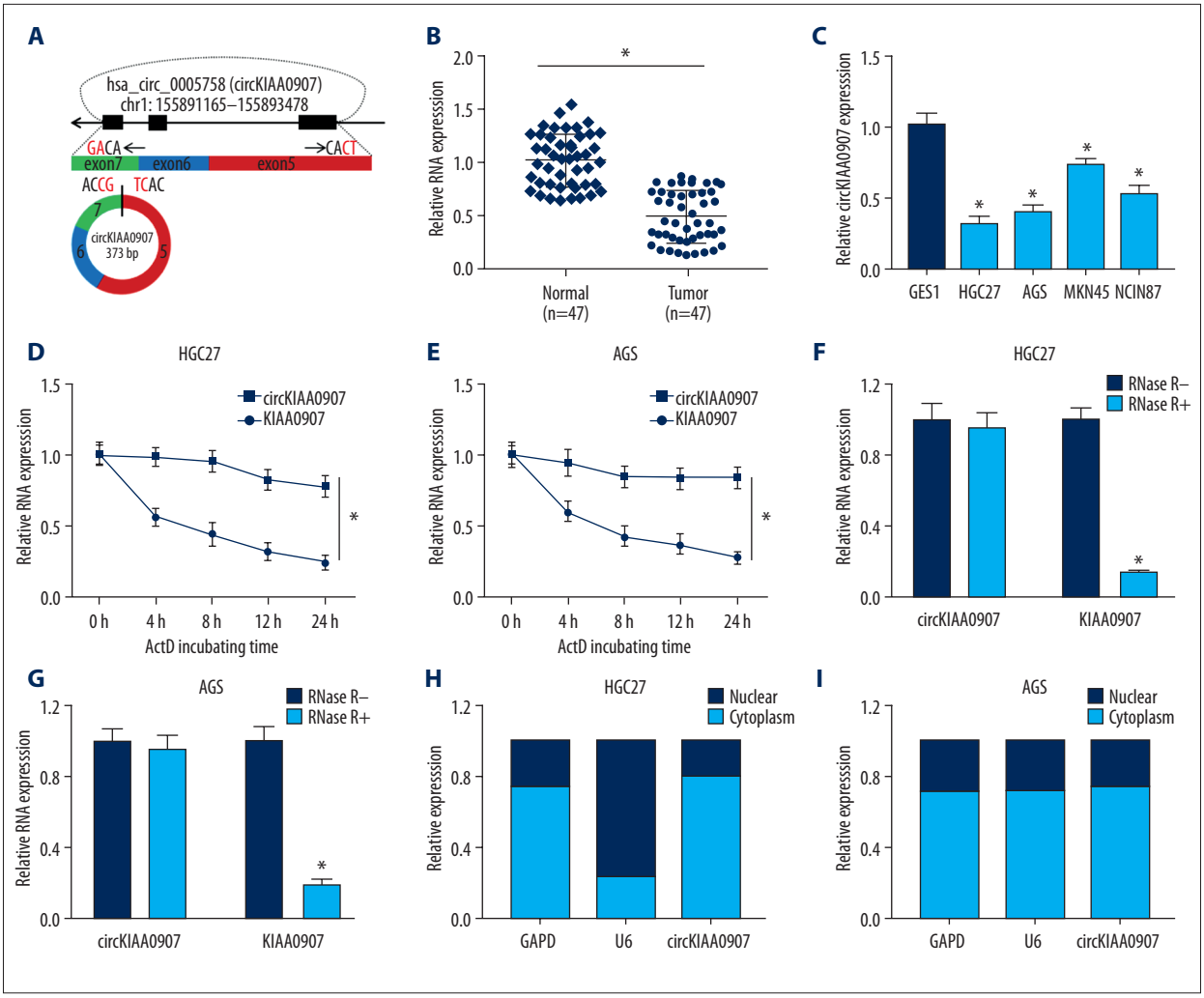

Figure 1. CircKIAA0907 expression was lessened in gastric cancer (GC) tissues and cells. (**A**) Genomic location of *KIAA0907* gene and circKIAA0907. (**B, C**) Level of circKIAA0907 was assayed using quantitative real-time polymerase chain reaction (qRT-PCR) in GC tissues (**B**) and cells (**C**). (**D–G**) qRT-PCR analysis of circKIAA0907 and KIAA0907 was implemented in HGC27 and AGS cells after treatment with actinomycin D (**D, E**) and RNase R (**F, G**). (**H, I**) CircKIAA0907 localization was analyzed through comparison with glyceraldehyde-3-phosphate dehydrogenase (GAPDH) and U6 via qRT-PCR detection. * $P<0.05$.

and miR-452-5p) pulled down by the circKIAA0907 probe (Figure 3C, 3D). We then found the binding sites of miR-452-5p in the sequence of circKIAA0907 through the prediction of circBank (Figure 3E). To confirm the direct combination of circKIAA0907 and miR-452-5p, we applied biotinylated-miR-452-5p to capture circKIAA0907. As shown in Figure 3F and 3G, biotin-miR-452-5p-WT pulled down more circKIAA0907 than biotin-miR-452-5p-MUT but failed to pull down GAPDH. A further dual-luciferase reporter assay also showed that miR-452-5p could bind to circKIAA0907 WT instead of circKIAA0907 MUT (Figure 3H, 3I). To study whether circKIAA0907 could affect miR-452-5p degradation, vector- or circKIAA0907-transfected HGC27 and AGS cells were treated with actinomycin D. As shown in the qRT-PCR result in Figure 3J and 3K, miR-452-5p in the circKIAA0907 group was markedly lower than that in the empty vector group at 12 h and 24 h posttreatment. Afterward, the expression of miR-452-5p in GC was determined. Both in tissues (Figure 3L) and in cells (Figure 3M), miR-452-5p was notably upregulated compared with their controls. Moreover, the inhibitory effect of circKIAA0907 overexpression on miR-452-5p levels was seen in HGC27 and AGS cells (Figure 3N, 3O). All these results clarified that circKIAA0907 served as a sponge for miR-452-5p in GC.

Increase of miR-452-5p reversed the inhibition of circKIAA0907 on the progression of GC cells

We then researched whether circKIAA0907 functioned as a tumor inhibitor by sponging miR-452-5p. The miR-452-5p mimic was shown to have great overexpression efficiency because its

This work is licensed under Creative Common Attribution-NonCommercial-NoDerivatives 4.0 International (CC BY-NC-ND 4.0)

Indexed in: [Current Contents/Clinical Medicine] [SCI Expanded] [ISI Alerting System] [ISI Journals Master List] [Index Medicus/MEDLINE] [EMBASE/Excerpta Medica] [Chemical Abstracts/CAS]

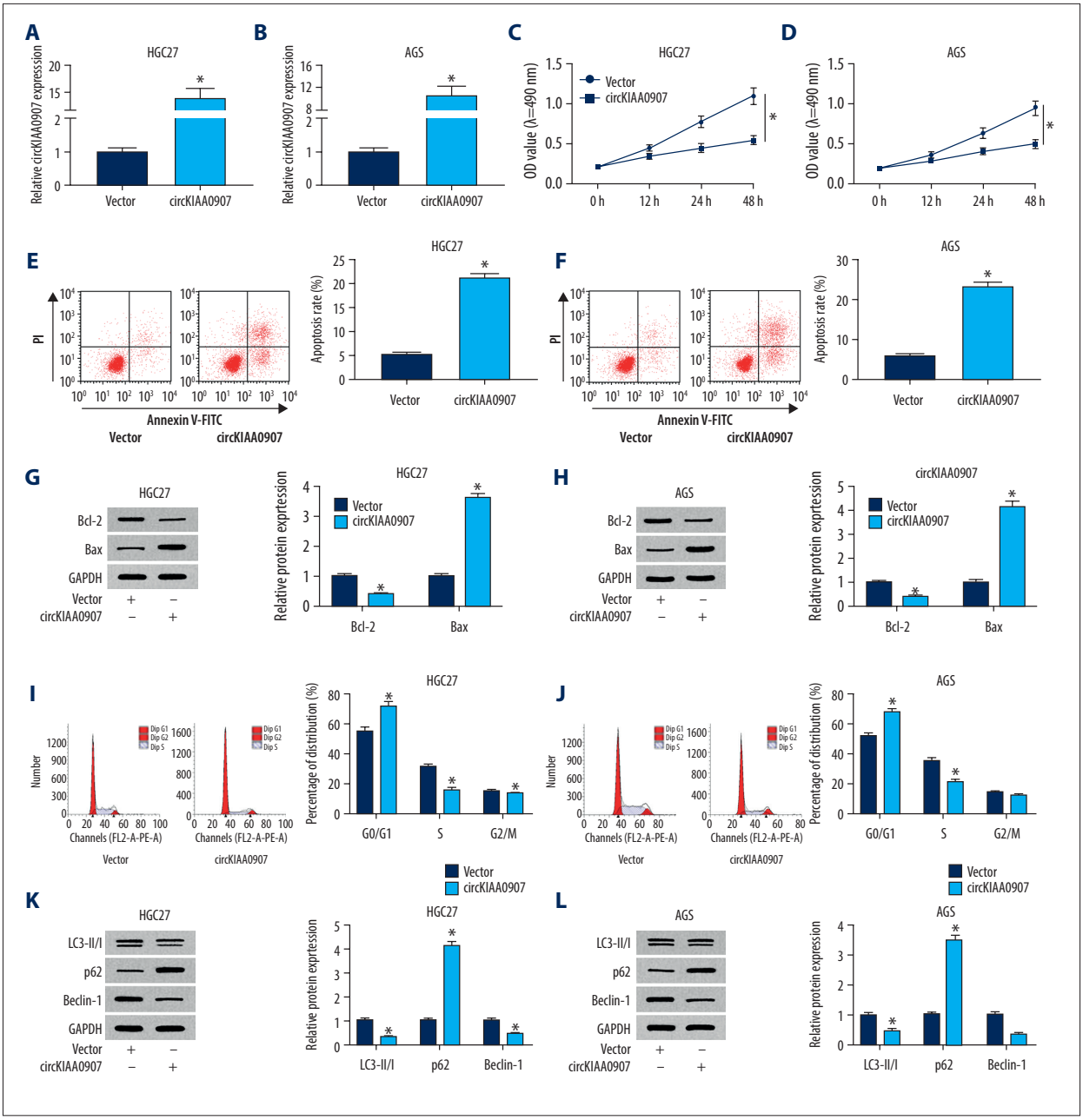

Figure 2. Overexpression of circKIAA0907 triggered proliferation and autophagy inhibition, cell cycle arrest, and apoptosis promotion of gastric cancer (GC) cells *in vitro*. (**A, B**) Evaluation of circKIAA0907 overexpression efficiency was conducted via quantitative real-time polymerase chain reaction (qRT-PCR) after transfection of vector or circKIAA0907. (**C, D**) Proliferation analysis in transfected GC cells was performed by 3-(4, 5-dimethylthiazol-2-y1)-2, 5-diphenyl tetrazolium bromide (MTT) assay. (**E, F**) Apoptosis rate of transfected cells was determined using flow cytometry. (**G, H**) Apoptosis-related proteins were assayed using western blot. (**I, J**) Cell cycle was analyzed via flow cytometry. (**K, L**) Western blot was used for detecting the autophagy-associated markers. * $P<0.05$.

introduction ameliorated the circKIAA0907-mediated miR-452-5p decrease (Figure 4A, 4B). Overtly, circKIAA0907 and miR-452-5p cotransfection induced cell proliferation (Figure 4C, 4D) and apoptosis inhibition (Figure 4E, 4F), in contrast to circKIAA0907 transfection alone. Western blot revealed that the changes of circKIAA0907 overexpression on Bcl-2 and Bax were relieved by miR-452-5p mimic (Figure 4G, 4H). After the transfection of miR-452-5p, the circKIAA0907-induced cell cycle arrest was also eliminated in part (Figure 4I, 4J). HGC27 and AGS cells cotransfected with circKIAA0907 and miR-452-5p expressed higher amounts

This work is licensed under Creative Common Attribution-NonCommercial-NoDerivatives 4.0 International (CC BY-NC-ND 4.0)

Indexed in: [Current Contents/Clinical Medicine] [SCI Expanded] [ISI Alerting System] [ISI Journals Master List] [Index Medicus/MEDLINE] [EMBASE/Excerpta Medica] [Chemical Abstracts/CAS]

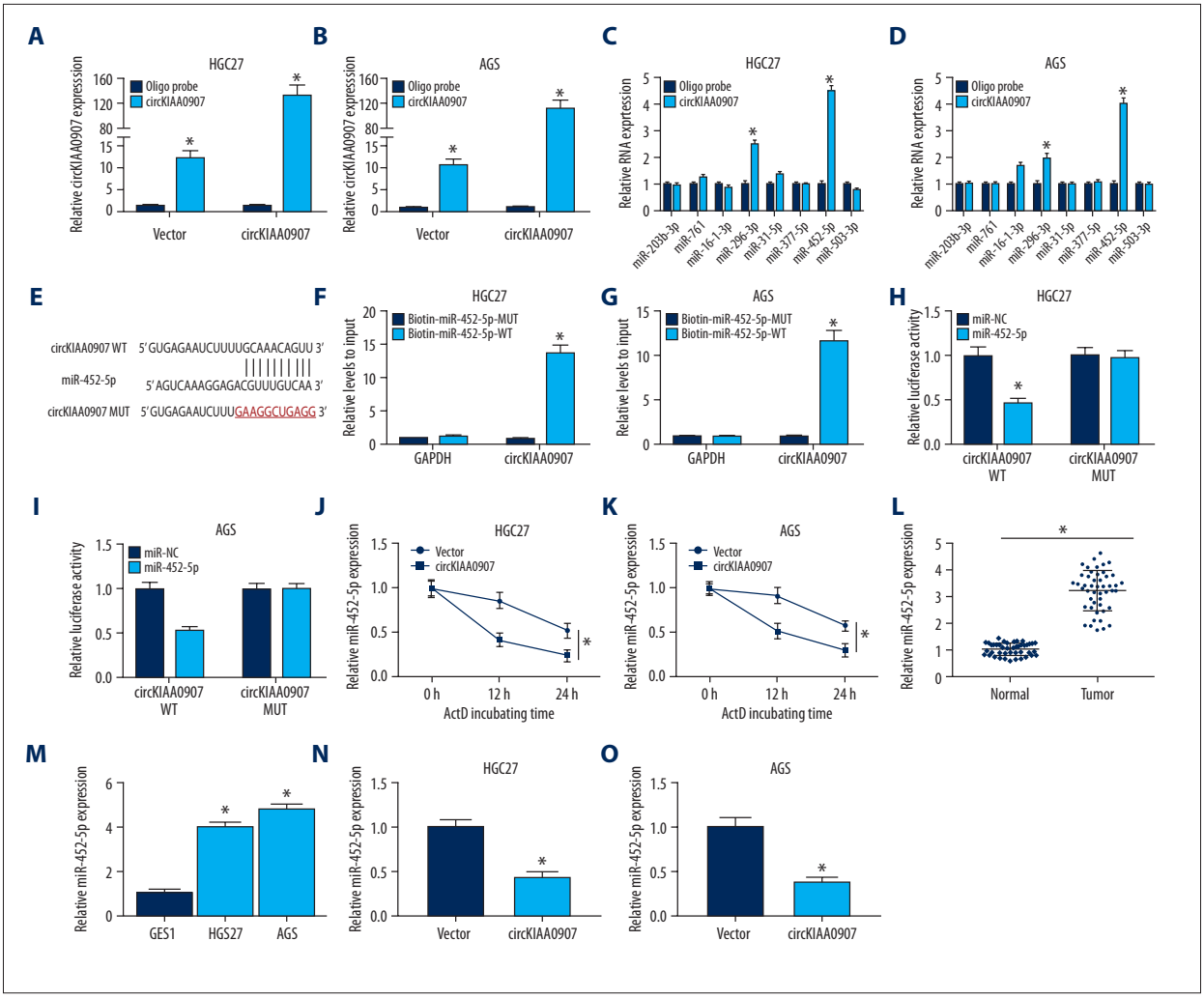

Figure 3. CircKIAA0907 could sponge miR-452-5p in gastric cancer (GC) cells. (**A, B**) Expression level of circKIAA0907 was analyzed by quantitative real-time polymerase chain reaction (qRT-PCR) after biotinylated-circKIAA0907 pull-down assay in HGC27 and AGS cells transfected with vector or circKIAA0907. (**C, D**) qRT-PCR was used to quantify the relative expression of candidate micro(mi)RNAs in HGC27 and AGS cells after administration of biotinylated-circKIAA0907 pull-down. (**E**) Binding sites of circKIAA0907 and miR-452-5p presented after analysis of circBank. (**F, G**) Pull-down assay was executed to prove the capture of circKIAA0907 by miR-452-5p. (**H, I**) Luciferase activities of transfected HGC27 and AGS cells were determined using the dual-luciferase reporter system. (**J, K**) MiR-452-5p level was examined using qRT-PCR after actinomycin D treatment at 0, 12, and 24 h in GC cells transfected with vector or circKIAA0907. (**L, M**) miR-452-5p was measured in GC tissues (**L**) and cells (**M**) by qRT-PCR. (**N, O**) MiR-452-5p level was determined through qRT-PCR after GC cells were transfected with vector or circKIAA0907. * $P<0.05$.

of LC3-II/I and Beclin-1 and lower amounts of p62 protein, in contrast with those cells transfected with circKIAA0907 solely (Figure 4K, 4L). The reverse of miR-452-5p to circKIAA0907 on inhibiting GC progression hinted that circKIAA0907 exerted an antitumor effect via sponging miR-452-5p.

CircKIAA0907 sponged miR-452-5p to elevate the expression of its target KAT6B

By carrying out the analysis of starBase v2.0, we discovered that the complementary sites of miR-452-5p were present in 3′-UTR of KAT6B (Figure 5A). Next, we implemented the dual-luciferase reporter assay, which showed that the luciferase activity of the recombinant vector containing the circKIAA0907 sequence was evidently suppressed by miR-452-5p overexpression, but that of the vector with mutant binding sites of miR-452-5p was almost insusceptible (Figure 5B, 5C). There was a stimulative effect on KAT6B protein levels caused by miR-452-5p inhibitor in HGC27 and AGS cells (Figure 5D), whereafter, upon western blot analysis, KAT6B was downregulated in GC tissue samples (Figure 5E) as well as in HGC27 and AGS cells (Figure 5F), in contrast to normal samples and GES-1 cell

This work is licensed under Creative Common Attribution-NonCommercial-NoDerivatives 4.0 International (CC BY-NC-ND 4.0)

Indexed in: [Current Contents/Clinical Medicine] [SCI Expanded] [ISI Alerting System] [ISI Journals Master List] [Index Medicus/MEDLINE] [EMBASE/Excerpta Medica] [Chemical Abstracts/CAS]

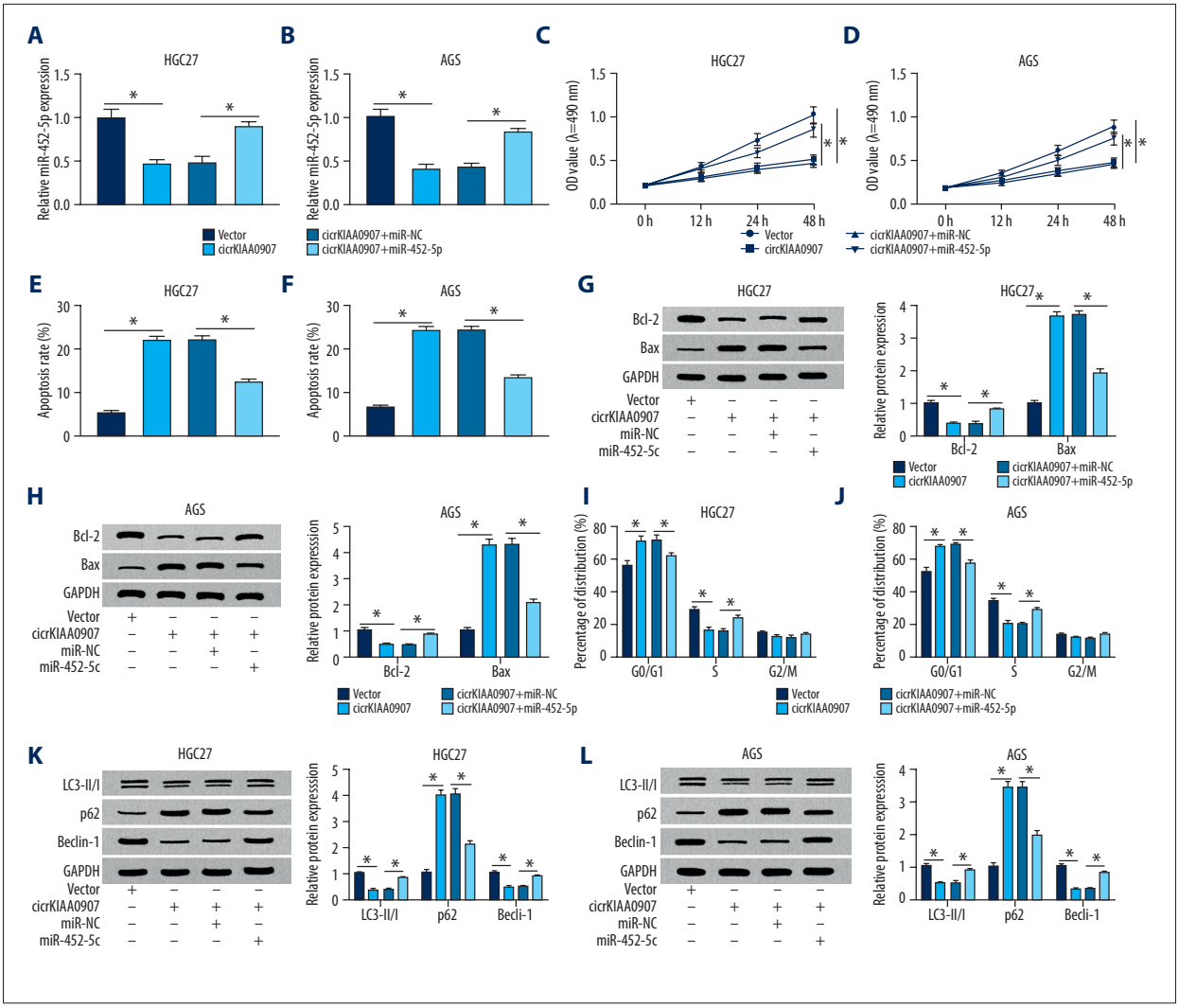

Figure 4. Increase of miR-452-5p reversed the inhibition of circKIAA0907 on the progression of gastric cancer (GC) cells. (**A, B**) After transfection of vector, circKIAA0907, circKIAA0907+miR-NC, and circKIAA0907+miR-452-5p in HGC27 and AGS cells, the expression of miR-452-5p was assayed via quantitative real-time polymerase chain reaction (qRT-PCR). (**C, D**) 3-(4, 5-Dimethylthiazol-2-y1)-2, 5-diphenyl tetrazolium bromide (MTT) assay was used for measuring proliferation ability in transfected cells. (**E–H**) Cell apoptosis was assessed with flow cytometry and western blot. (**I, J**) The percentage of each phase in transfected GC cells was examined by cell cycle detection. (**K, L**) Evaluation of autophagy was carried out by detecting associated proteins after western blot. * $P<0.05$.

line. Of more interest, circKIAA0907 led to the promotion of KAT6B protein expression, whereas miR-452-5p transfection counteracted this effect (Figure 5G). These data show that *KAT6B* was a target of miR-452-5p and circKIAA0907 enhanced KAT6B expression by sponging miR-452-5p.

CircKIAA0907 worked as a tumor repressor in GC progression via miR-452-5p-mediated KAT6B upregulation

After discovering the target relation of miR-452-5p to KAT6B, we further researched their effects on cellular processes of GC cells. In western blot assay, si-*KAT6B* transfection returned the anti-miR-452-5p-induced elevation of KAT6B protein level in HGC27 and AGS cells, indicating that siRNA-mediated KAT6B knockdown was obvious (Figure 6A, 6B). HGC27 and AGS cells transfected with anti-miR-452-5p exhibited decreased proliferation ability (Figure 6C, 6D) and accelerated apoptosis (Figure 6E, 6F) and the alteration of apoptosis proteins (the downregulation of Bcl-2 and promotion of Bax) (Figure 6G, 6H); the introduction of si-KAT6B neutralized these effects. In addition, the blockage of the transition from G0/G1 to S phase caused by miR-452-5p inhibitor was also weakened after knockdown of KAT6B (Figure 6I, 6J). The reduction of LC3B-II/I and Beclin-1 and increase of p62 triggered by the

This work is licensed under Creative Common Attribution-NonCommercial-NoDerivatives 4.0 International (CC BY-NC-ND 4.0)

Indexed in: [Current Contents/Clinical Medicine] [SCI Expanded] [ISI Alerting System] [ISI Journals Master List] [Index Medicus/MEDLINE] [EMBASE/Excerpta Medica] [Chemical Abstracts/CAS]

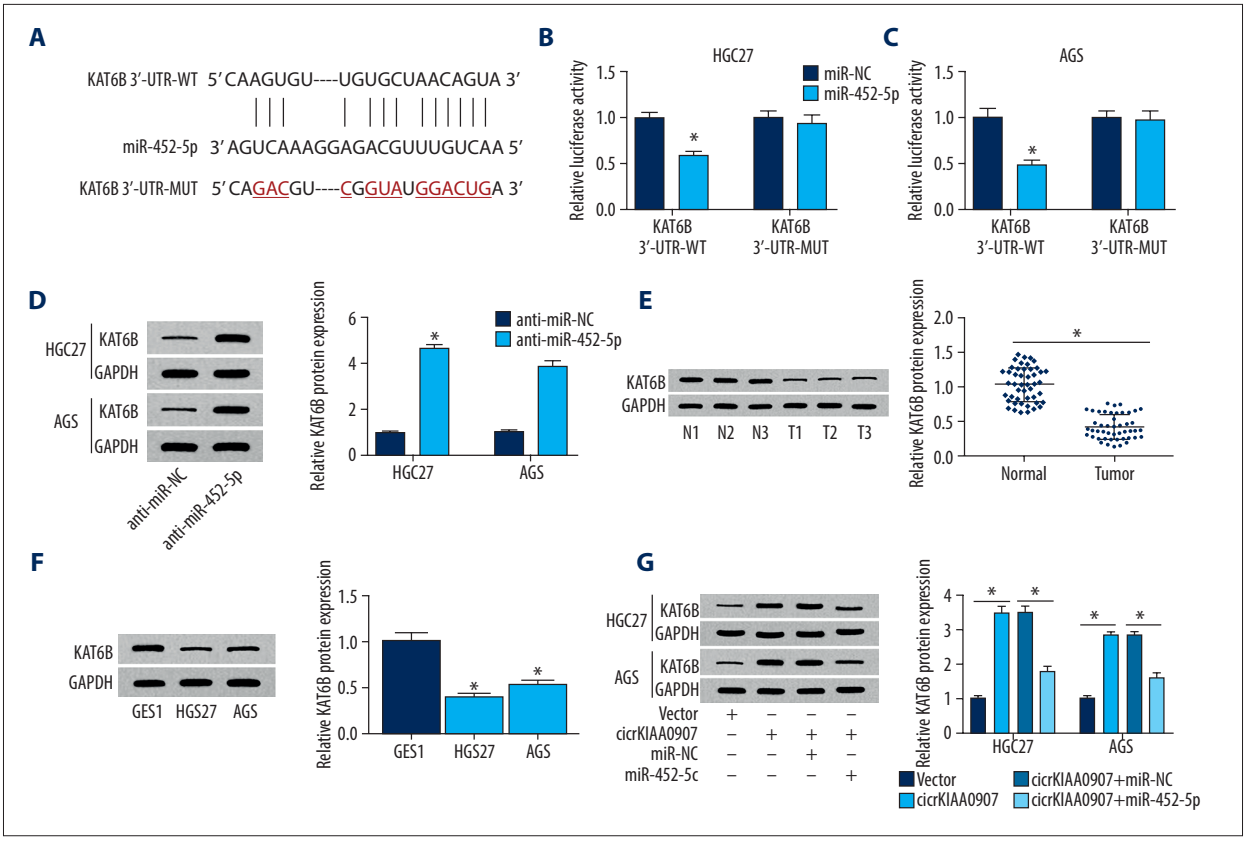

Figure 5. CircKIAA0907 sponged miR-452-5p to elevate expression of its target KAT6B. (**A**) The starbase v2.0 was utilized for analyzing the binding sites of KAT6B 3′-UTR and miR-452-5p. (**B, C**) The dual-luciferase reporter assay was used to determine whether miR-452-5p interacted with KAT6B. (**D**) The impact of anti-miR-452-5p on KAT6B was assayed using western blot. (**E, F**) Analysis of KAT6B level in gastric cancer (GC) tissues (**E**) and cells (**F**) via western blot. (**G**) After the respective transfection of circKIAA0907, circKIAA0907+miR-452-5p, or relative controls in HGC27 and AGS cells, the protein expression of KAT6B was determined via western blot. * $P<0.05$.

downregulation of miR-452-5p were all recovered after the co-transfection of anti-miR-452-5p and si-KAT6B (Figure 6K, 6L). Furthermore, KAT6B knockdown was also shown to counterbalance the circKIAA0907-induced cell proliferation inhibition, cell cycle arrest, and apoptosis increase in GC cells (Supplementary Figure 1). Thus, we concluded that circKIAA0907 played a tumor-inhibitory role in the development of GC via the miR-452-5p-mediated expression promotion.

CircKIAA0907 inhibited tumorigenesis of GC *in vivo* via the miR-452-5p/KAT6B axis

We established a xenograft model to ascertain the anticancer role of circKIAA0907 *in vivo*. It was apparent that tumor volume decreased after injection of HGC27 and AGS cells transfected with circKIAA0907 (relative to empty vector transfection) (Figure7A). The same phenomenon was observed in the weight of excised tumors (Figure 7B, 7C). Additionally, circKIAA0907 and KAT6B (mRNA and protein) were shown to increase in rhe circKIAA0907 group, whereas miR-452-5p was downregulated in comparison with the vector group after qRT-PCR and western blot analysis (Figure 7D, 7E). Altogether, circKIAA0907 inhibited GC tumor growth *in vivo* by enhancing KAT6B expression via sponging miR-452-5p.

Discussion

It has become increasingly crucial to understand the pathogenic mechanism and discover useful molecular targets to improve early diagnosis and late treatment for GC. In the current study, circKIAA0907 was identified as a tumor-promoting factor in GC for the first time and its functional mechanism based on the regulation of miR-452-5p/KAT6B was also first revealed here, showing the potential of circKIAA0907 as an available biological target for GC.

CircRNAs are formed by nonclassical backsplicing of pre-mRNAs with no free 3′ polyadenylate tail or 5′ cap in mammalian cells for high stability and conservation [19]. Consistently,

This work is licensed under Creative Common Attribution-NonCommercial-NoDerivatives 4.0 International (CC BY-NC-ND 4.0)

Indexed in: [Current Contents/Clinical Medicine] [SCI Expanded] [ISI Alerting System] [ISI Journals Master List] [Index Medicus/MEDLINE] [EMBASE/Excerpta Medica] [Chemical Abstracts/CAS]

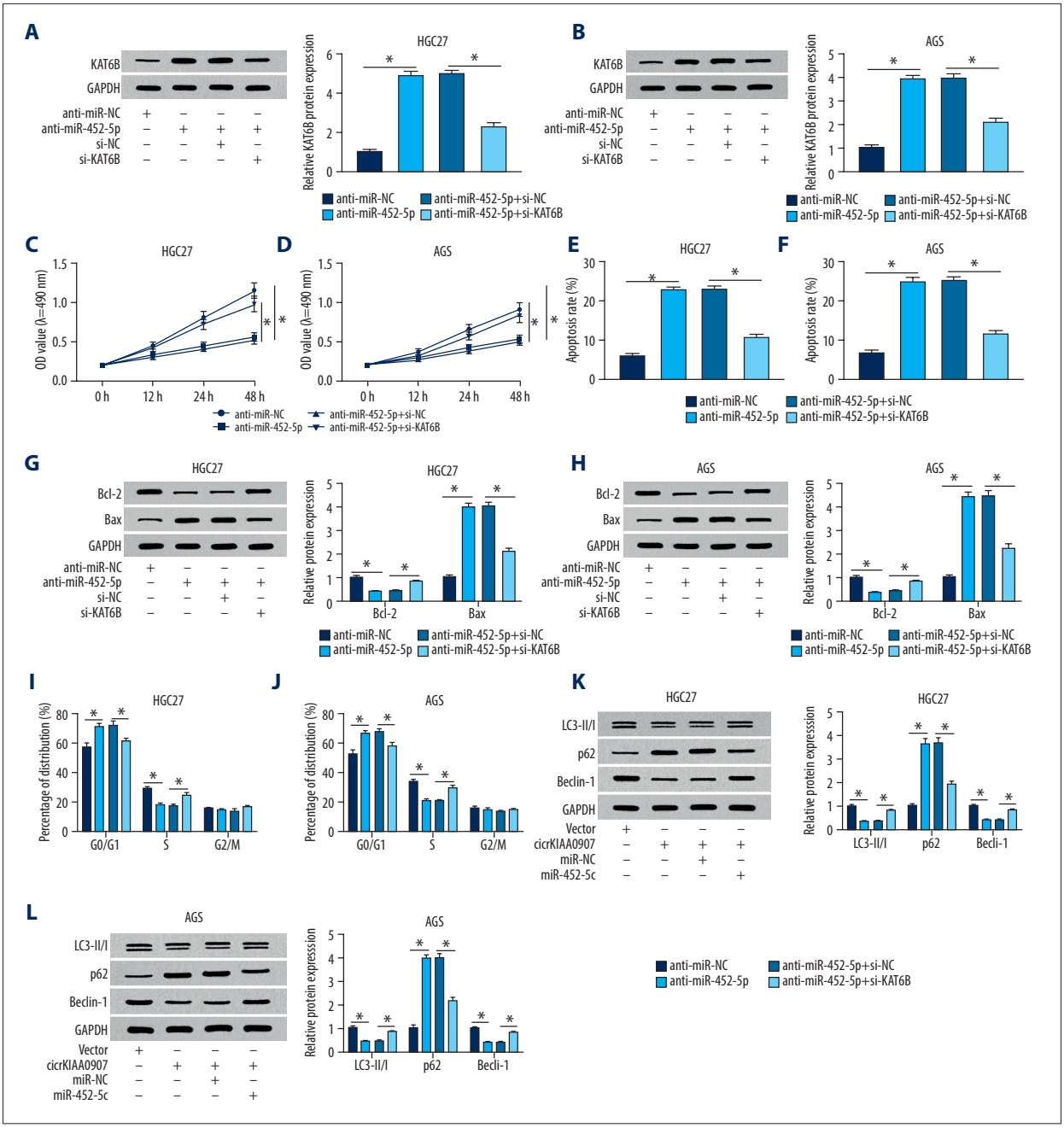

Figure 6. CircKIAA0907 worked as a tumor repressor in gastric cancer (GC) progression via the miR-452-5p-mediated KAT6B upregulation. (**A, B**) KAT6B was measured using western blot in HGC27 and AGS cells transfected with anti-miR-NC, anti-miR-452-5p, anti-miR-452-5p+si-NC, or anti-miR-452-5p+si-KAT6B. (**C, D**) Examination of proliferation ability in transfected cells implemented through 3-(4, 5-dimethylthiazol-2-y1)-2, 5-diphenyl tetrazolium bromide (MTT) assay. (**E–H**) Flow cytometry and western blot to evaluate cell apoptosis. (**I, J**) Cell cycle analysis using flow cytometry. (**K, L**) Cellular autophagy assessed utilizing western blot. * $P<0.05$.

This work is licensed under Creative Common Attribution-NonCommercial-NoDerivatives 4.0 International (CC BY-NC-ND 4.0)

Indexed in: [Current Contents/Clinical Medicine] [SCI Expanded] [ISI Alerting System] [ISI Journals Master List] [Index Medicus/MEDLINE] [EMBASE/Excerpta Medica] [Chemical Abstracts/CAS]

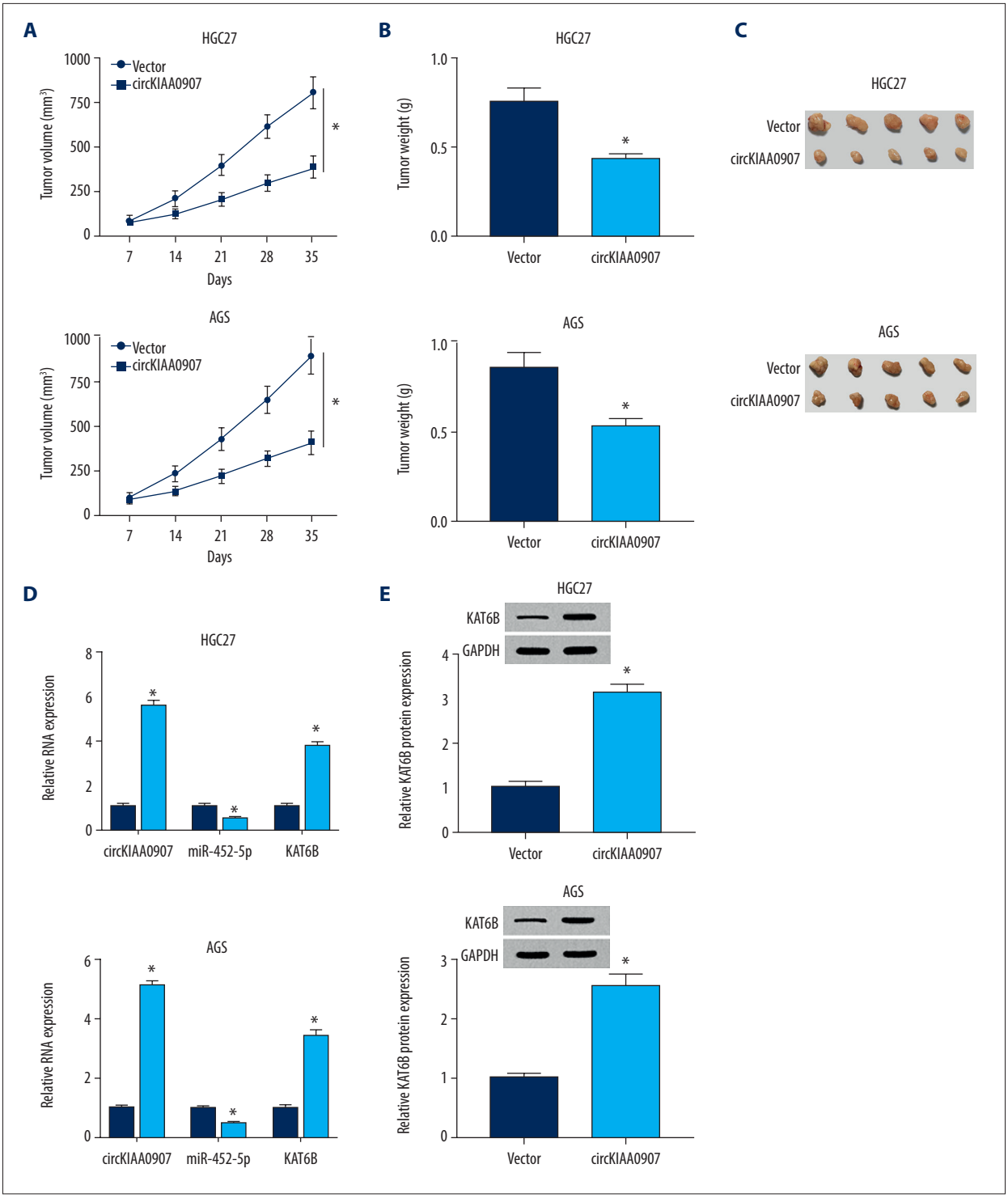

Figure 7. CircKIAA0907 inhibited tumorigenesis of gastric cancer (GC) *in vivo* via the miR-452-5p/KAT6B axis. (**A**) Tumor volume was recorded weekly after injecting HGC27 and AGS cells transfected with circKIAA0907 or vector. (**B, C**) Tumors were weighed (**B**) after excision from mice (**C**). (**D**) Quantitative real-time polymerase chain reaction (qRT-PCR) was used for examining expression of *circKIAA0907*, miR-452-5p, and *KAT6B* mRNA. (**E**) KAT6B protein level detected using western blot. * $P<0.05$.

This work is licensed under Creative Common Attribution-NonCommercial-NoDerivatives 4.0 International (CC BY-NC-ND 4.0)

Indexed in: [Current Contents/Clinical Medicine] [SCI Expanded] [ISI Alerting System] [ISI Journals Master List] [Index Medicus/MEDLINE] [EMBASE/Excerpta Medica] [Chemical Abstracts/CAS]

circKIAA0907 in this study was more stable than linear KIAA0907 after actinomycin D and RNase R treatment in GC cells. Zhang et al. showed that knockdown of circNRIP1 hampered GC cell proliferation, migration, and invasion via serving as the sponge of miR-149-5p to mediate the AKT1/mTOR pathway [20]. Circ-DONSON promoted cell growth and invasion in GC by upregulating SOX4 [21]. On the contrary, there were several circRNAs having antitumor effects on GC. For example, circLARP4 elevated LATS1 to inhibit cell proliferation and invasion in GC cells via miR-424-5p repression [22]; circYAP1 was reported to be a repressive factor in GC progression via the regulation of miR-367-5p/p27 axis [23].

After verifying the aberrant downregulation of circKIAA0907 in GC tissues and cells, we performed a series of experiments *in vitro* to study its effects on GC cellular behaviors. The results suggested that circKIAA0907 inhibited cell proliferation, cell cycle, and autophagy, and promoted apoptosis in two GC cell lines, thus acting as a tumor inhibitor. Interestingly, autophagy (a well-known intracellular homeostatic catabolic pathway) has both pro-survival and pro-apoptotic effects on tumor cells, including GC [24,25]. Herein, circKIAA0907 was found to inhibit tumors in GC via blocking autophagy.

MiR-452-5p is less studied but the research has indicated its vital role in cancer regulation. For instance, Gao et al. asserted that miR-452-5p was downregulated and associated with tumorigenesis inhibition of prostate cancer [26], whereas Gan et al. found the ectopic high level of miR-452-5p and its pro-cancer role in lung squamous cell carcinoma [27]. In the current report, miR-452-5p was verified to be overexpressed in GC, and a miR-452-5p inhibitor strikingly caused proliferation and autophagy suppression, cell cycle arrest, and apoptosis enhancement of GC cells, which implied that miR-452-5p functioned as an oncogene in GC. CircRNAs are usually regarded as miRNA sponges in different human cancers [28]. By conducting RNA pull-down assays, only miR-452-5p was largely pulled down by a circKIAA0907 probe. We then confirmed that circKIAA0907 could directly sponge the endogenous miR-452-5p to exert its suppressive influence on the oncogenesis of GC *in vitro*.

Additionally, *KAT6B* was identified to be a target gene of miR-452-5p in GC cells. MiR-452-5p exerted its function by negatively regulating *KAT6B*. Mounting data have indicated that circRNAs regulated the miRNA-mRNA axis to affect tumor occurrence and progression in multiple cancers [29,30], certainly including GC [31,32]. In our study, circKIAA0907 had a similar positive regulation on KAT6B expression as a miR-452-5p sponge in GC cells, and KAT6B downregulation could restore the effects of circKIAA0907 on GC cells. *In vivo*, circKIAA0907 overexpression also impeded GC tumorigenesis via action on the miR-452-5p/KAT6B axis.

Conclusions

Through functional analysis, circKIAA0907 was affirmed as a new type of antitumor circRNA in GC. By performing recovery assays, we proved the existence of a circKIAA0907/miR-452-5p/KAT6B axis in regulating GC progression. CircKIAA0907 may have significant value in clinical screening, diagnosis, and prognosis. Regarding clinical treatment, circKIAA0907 upregulation will be a useful therapeutic strategy to fight GC.

Availability of data and materials

The analyzed data sets generated during the present study are available from the corresponding author upon request.

Confiuct of interests

None.

This work is licensed under Creative Common Attribution-NonCommercial-NoDerivatives 4.0 International (CC BY-NC-ND 4.0)

Indexed in: [Current Contents/Clinical Medicine] [SCI Expanded] [ISI Alerting System] [ISI Journals Master List] [Index Medicus/MEDLINE] [EMBASE/Excerpta Medica] [Chemical Abstracts/CAS]

Supplementary Data

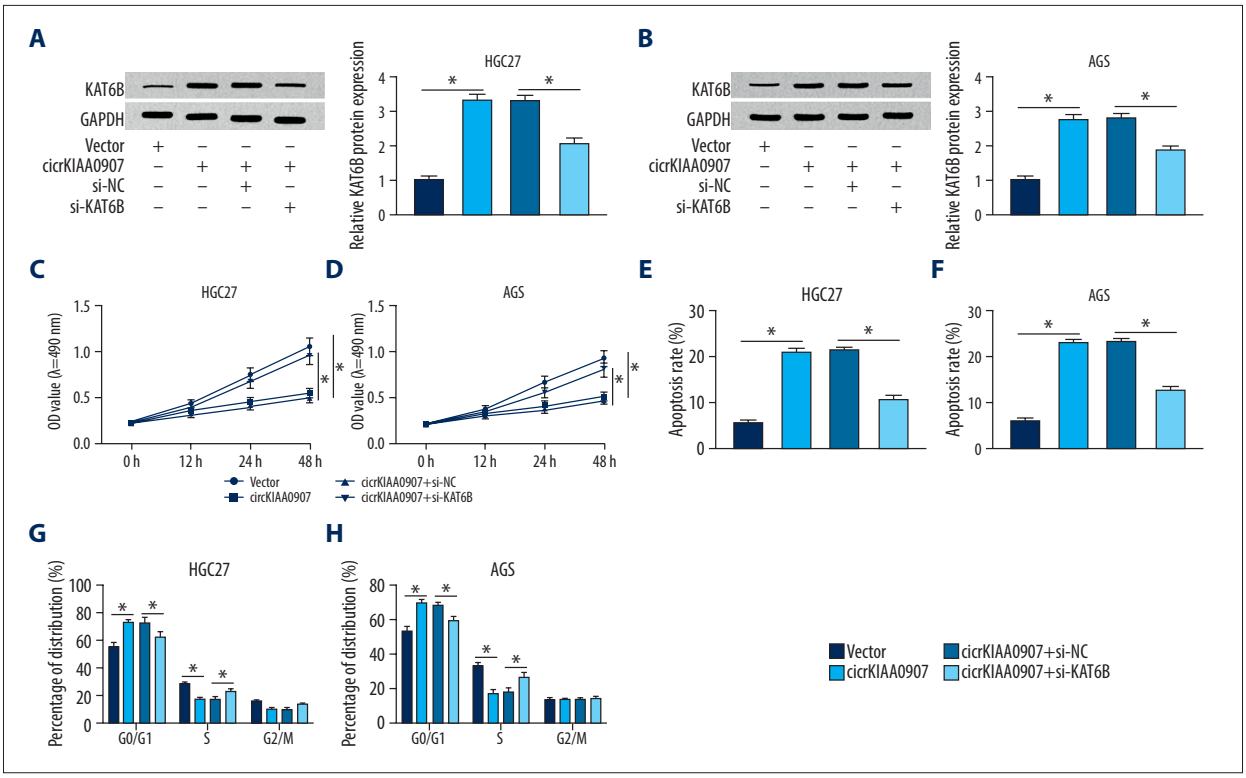

Supplementary Figure 1. KAT6B knockdown rescued the tumor-inhibitory effect of circKIAA0907 on gastric cancer (GC) cells. (**A, B**) After transfection of vector, circKIAA0907, circKIAA0907+si-NC, or circKIAA0907+si-KAT6B, western blot was used to determine KAT6B protein level in HGC27 and AGS cells. (**C, D**) Cell proliferation measured by 3-(4, 5-dimethylthiazol-2-y1)-2, 5-diphenyl tetrazolium bromide (MTT) assay. (**E–H**) Analyses of cell apoptosis (**E, F**) and cell cycle (**G, H**) via flow cytometry. * $P<0.05$.

References:

1. Bray F, Ferlay J, Soerjomataram I et al: Global cancer statistics 2018: GLOBOCAN estimates of incidence and mortality worldwide for 36 cancers in 185 countries. Cancer J Clin, 2018; 68(6): 394–424
2. Digklia A, Wagner AD: Advanced gastric cancer: Current treatment landscape and future perspectives. World J Gastroenterol, 2016; 22(8): 2403–14
3. Figueiredo C, Camargo MC, Leite M et al: Pathogenesis of gastric cancer: Genetics and molecular classification. Curr Top Microbiol Immunol, 2017; 400: 277–304
4. Chen B, Huang S: Circular RNA: An emerging non-coding RNA as a regulator and biomarker in cancer. Cancer Lett, 2018; 418: 41–50
5. Zhao ZJ, Shen J: Circular RNA participates in the carcinogenesis and the malignant behavior of cancer. RNA Biol, 2017; 14(5): 514–21
6. Li Y, Zhang J, Pan S et al: CircRNA CDR1as knockdown inhibits progression of non-small-cell lung cancer by regulating miR-219a-5p/SOX5 axis. Thorac Cancer, 2020; 11(3): 537–48
7. Lin L, Cai J: Circular RNA circ-EGLN3 promotes renal cell carcinoma proliferation and aggressiveness via miR-1299-mediated IRF7 activation. J Cell Biochem, 2020 [Online ahead of print]
8. Lin W, Ye H, You K et al: Up-regulation of circ_LARP4 suppresses cell proliferation and migration in ovarian cancer by regulating miR-513b-5p/LARP4 axis. Cancer Cell Int, 2020; 20: 5
9. Fan M, Wang Y, Gao S: Circular RNA circMTO1 acts as an antitumor factor in rectal cancer cell lines by downregulation of miR-19b-3p. J Cell Biochem, 2019 [Online ahead of print]
10. Shao Y, Li J, Lu R et al: Global circular RNA expression profile of human gastric cancer and its clinical significance. Cancer Med, 2017; 6(6): 1173–80
11. Lu R, Shao Y, Tao X et al: Clinical significances of hsa_circ_0067582 and hsa_circ_0005758 in gastric cancer tissues. J Clin Lab Anal, 2019; 33(9): e22984
12. Hammond SM: An overview of microRNAs. Adv Drug Deliv Rev, 2015; 87: 3–14
13. Panda AC: Circular RNAs act as miRNA sponges. Adv Exp Med Biol, 2018; 1087: 67–79
14. He X, Shu Y: miR-452 promotes the development of gastric cancer via targeting EPB41L3. Pathol Res Pract, 2020; 216(1): 152725
15. He W, Zhang MG, Wang XJ et al: KAT5 and KAT6B are in positive regulation on cell proliferation of prostate cancer through PI3K-AKT signaling. Int J Clin Exp Pathol, 2013; 6(12): 2864–71
16. Simo-Riudalbas L, Perez-Salvia M, Setien F et al: KAT6B is a tumor suppressor histone H3 lysine 23 acetyltransferase undergoing genomic loss in small cell lung cancer. Cancer Res, 2015; 75(18): 3936–45
17. Ding H, Shi Y, Liu X et al: MicroRNA-4513 promotes gastric cancer cell proliferation and epithelial-mesenchymal transition through targeting KAT6B. Hum Gene Ther Clin Dev, 2019; 30(3): 142–48
18. Bortnik S, Gorski SM: Clinical applications of autophagy proteins in cancer: From potential targets to biomarkers. Int J Mol Sci, 2017; 18(7): 1496
19. Jeck WR, Sharpless NE: Detecting and characterizing circular RNAs. Nat Biotechnol, 2014; 32(5): 453–61

This work is licensed under Creative Common Attribution-NonCommercial-NoDerivatives 4.0 International (CC BY-NC-ND 4.0)

Indexed in: [Current Contents/Clinical Medicine] [SCI Expanded] [ISI Alerting System] [ISI Journals Master List] [Index Medicus/MEDLINE] [EMBASE/Excerpta Medica] [Chemical Abstracts/CAS]

20. Zhang X, Wang S, Wang H et al: Circular RNA circNRIP1 acts as a microRNA-149-5p sponge to promote gastric cancer progression via the AKT1/mTOR pathway. Mol Cancer, 2019; 18(1): 20
21. Ding L, Zhao Y, Dang S et al: Circular RNA circ-DONSON facilitates gastric cancer growth and invasion via NURF complex dependent activation of transcription factor SOX4. Mol Cancer, 2019; 18(1): 45
22. Zhang J, Liu H, Hou L et al: Circular RNA_LARP4 inhibits cell proliferation and invasion of gastric cancer by sponging miR-424-5p and regulating LATS1 expression. Mol Cancer, 2017; 16(1): 151
23. Liu H, Liu Y, Bian Z et al: Circular RNA YAP1 inhibits the proliferation and invasion of gastric cancer cells by regulating the miR-367-5p/p27 (Kip1) axis. Mol Cancer, 2018; 17(1): 151
24. Qian HR, Yang Y: Functional role of autophagy in gastric cancer. Oncotarget, 2016; 7(14): 17641–51
25. Cao Y, Luo Y, Zou J et al: Autophagy and its role in gastric cancer. Clin Chim Acta, 2019; 489: 10–20
26. Gao L, Zhang LJ, Li SH et al: Role of miR-452-5p in the tumorigenesis of prostate cancer: A study based on the cancer genome Atl(TCGA), gene expression omnibus (GEO), and bioinformatics analysis. Pathol Res Pract, 2018; 214(5): 732–49
27. Gan XN, Gan TQ, He RQ et al: Clinical significance of high expression of miR-452-5p in lung squamous cell carcinoma. Oncol Lett, 2018; 15(5): 6418–30
28. Meng S, Zhou H, Feng Z et al: CircRNA: Functions and properties of a novel potential biomarker for cancer. Mol Cancer, 2017; 16(1): 94
29. Tong H, Zhao K, Wang J et al: CircZNF609/miR-134-5p/BTG-2 axis regulates proliferation and migration of glioma cell. J Pharm Pharmacol, 2020; 72(1): 68–75
30. Xiong DD, Dang YW, Lin P et al: A circRNA-miRNA-mRNA network identification for exploring underlying pathogenesis and therapy strategy of hepatocellular carcinoma. J Transl Med, 2018; 16(1): 220
31. Liu T, Liu S, Xu Y et al: Circular RNA-ZFR inhibited cell proliferation and promoted apoptosis in gastric cancer by sponging miR-130a/miR-107 and modulating PTEN. Cancer Res Treat, 2018; 50(4): 1396–417
32. Cheng J, Zhuo H, Xu M et al: Regulatory network of circRNA-miRNA-mRNA contributes to the histological classification and disease progression in gastric cancer. J Transl Med, 2018; 16(1): 216

This work is licensed under Creative Common Attribution-NonCommercial-NoDerivatives 4.0 International (CC BY-NC-ND 4.0)

Indexed in: [Current Contents/Clinical Medicine] [SCI Expanded] [ISI Alerting System] [ISI Journals Master List] [Index Medicus/MEDLINE] [EMBASE/Excerpta Medica] [Chemical Abstracts/CAS]